Lasers in Manufacturing Conference 2017

Heat accumulation effects on efficiency during laser drilling of metals

Daniel J. Förster[a,b,*], Rudolf Weber[b], Thomas Graf[a,b]

[a] *Graduate School of advanced Manufacturing Engineerging GSaME, Nobelstrasse 12, 70569 Stuttgart, Germany*
[b] *Institut für Strahlwerkzeuge IFSW, Pfaffenwaldring 43, 70569 Stuttgart, Germany*

Abstract

Pulsed laser materials processing with pulse durations <10 ps might lead to direct sublimation or evaporation of the material resulting in very small thermal damage. However, it was shown that for Cu, Mg, Au, and Si the thermal load might be significant even for 60 fs pulses. The thermalized energy after the ablation process which remains within the material normalized by the applied energy is the so called "residual heat". The residual heat in multi-pulse processing of different materials with ultrashort pulses was investigated at low repetition rates for Al, Zn, and Pt and under influence of different environment.
As multi-pulse processing is gaining importance in the industry, recent studies of the effects of residual heat concentrated on the processing of steel with respect to heat accumulation at higher repetition rates.
Results of residual heat measurements during laser drilling of steel sheets of up to 1.5 mm thickness are discussed in the following. The pulse duration of the laser system was 10 ps, the repetition rate was varied in the range from 10 kHz to 300 kHz at constant pulse energy.

Keywords: Residual heat; Heat accumulation; Percussion drilling; Steel

1. Introduction

The ablation induced by ultra-short pulses with durations from femto- (fs) to picoseconds (ps) in general is dominated by direct evaporation of the irradiated material (Chichkov et al, 1996). One implication of this circumstance is that a much smaller amount of energy remains in the material after the ablation process compared to ablation with pulses with durations of nanoseconds (ns) and longer. This behavior is often referred to as “cold ablation” (Cheng et al., 2013, Hada et al., 2014) or “non-thermal ablation” (Loesel, 1998, Yang et al., 2007).

In 2005, Vorobyev et al. showed that the fraction of remaining energy (called residual heat in the following) in aluminum after single pulse ablation with pulses with durations of several 10 ns and 60 fs is of the

same amount, i.e. around 25% to 35% for fluences close to the ablation threshold. Furthermore, they concluded that for a 60 fs pulse the fraction of residual heat can increase to 70% for high fluences (100 times the ablation threshold). The studies of Vorobyev et al. as well as Bulgakova et al. later focused on the influence of vacuum (2005, 2006) and different gas media at various pressures (2008) on the fraction of residual heat when processing several metals. All these studies were done by using ultra-short pulsed lasers with repetition rates ≤ 1 kHz.

Recently, the fraction of residual heat and the corresponding heat accumulation effects when using high repetitive lasers again gained attraction in the field of micro machining with ultrafast lasers (Bauer et al., 2015, Weber et al. 2014 and 2017).

For the quantification of the fraction of residual heat during the laser drilling process with ultrafast lasers at repetition rates between 10 kHz and 300 kHz, experiments were performed. They are presented in the following.

2. Experimental procedures

2.1. Calorimetric measurement

To investigate the fraction of residual heat for different processing parameters, a calorimetric setup has been used as sketched in in Fig. 1). A copper substrate is connected to a 4-wire PT 100 thermal sensor on its bottom. The thermal sensor is connected to a data acquisition system (USB-2401, ADLINK technology) and a PC for analysis. On the top of the substrate, steel samples of different thickness were placed. By using different thicknesses we were able to vary the mass of the system. All described pieces were linked by using thermal heatsink paste (Arctic Silver 5, Arctic Silver). The copper substrate was held by plastic screws to thermally isolate the sample system. Another plastic screw was used to press the thermal sensor to the bottom of the copper plate. All screws were held by a surrounding sample holder made of aluminum.

Laser pulses were applied to the top of the steel sample. The laser beam was positioned by a galvanometer scanner (Scanlab IntelliScan 20) which focused the incoming laser beam by telecentric optics to a focal diameter of 20 µm. The used laser system (Trumpf TruMicro 5050) emitted pulses with 8 ps pulse duration and a wavelength of 1030 nm. The maximum repetition rate was 300 kHz which could be decreased at constant energy. The maximum power was 77 W, hence the maximum pulse energy was 255 µJ.

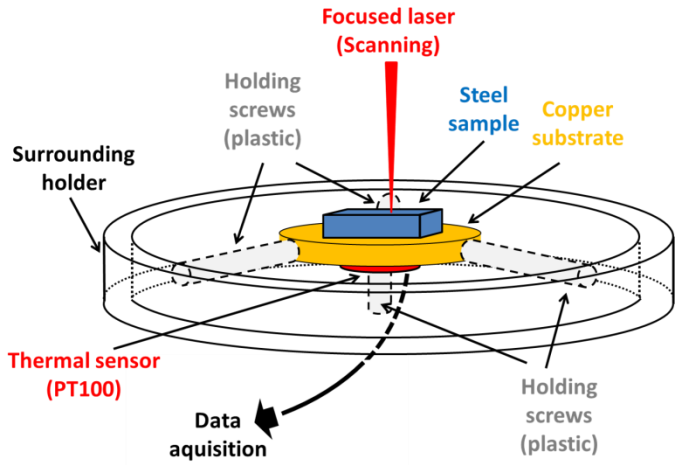

Fig. 1. Schematic view of the calorimetric setup used for the experiments.

The calorimetric measurements were done according to the Norm ISO 11551 by the so-called pulse procedure. The characteristic heating times of the sample were 10 to 30 seconds. The error introduced by the measurement of the relative temperature increase was <1.5% when heating up the sample by 5 degrees or more. To guarantee this minimum needed temperature increase, different sample thicknesses and drilling times were used. For long drilling times in the range of seconds, only drilling of a single hole accounted for this temperature increase. If the drilling times were in the range of several milliseconds, several hundred holes had to be drilled to achieve the required temperature increase. The positioning time was 400 µs therefore much shorter than the drilling times.

The temperature difference ΔT was used to determine the increase of the internal energy ΔE of the sample. For this purpose the masses m_i of the copper and steel plate were determined by a precision balance. The specific heat capacities $C_{P,i}$ were taken from material data sheets of the supplier. The rise of the internal energy corresponds to the residual heat and can be calculated by

$$\Delta E = \Delta T \cdot \sum_i m_i \cdot C_{P,i} \quad . \qquad (1)$$

The fraction of residual heat that remains in the sample after the drilling process can be calculated by taking the applied energy into account, which is given by $E_{in} = P_{Laser} \cdot t_{drilling,tot} = P_{Laser} \cdot t_{drilling} \cdot N_{holes}$. The fraction of residual heat η_{res} is then given by

$$\eta_{\mathrm{res}} = \frac{\Delta E}{E_{in}} = \frac{\Delta T \cdot \sum_i m_i \cdot C_{P,i}}{P_{Laser} \cdot t_{drilling} \cdot N_{holes}} \quad . \qquad (2)$$

2.2. Qualification of the calorimetric measurement

The residual energy coefficient represents the relative amount of energy that remains in the workpiece after processing and can take values between 0 and 1. If the applied laser fluence is below the ablation threshold, this value is equal to the absorptivity of the material.

For the qualification of the setup, the absorptivity of polished copper and steel samples have been determined, cf. table 1. Furthermore, by positioning the sample at different angles, the Fresnel equations could be

fitted and hence, the refractive indices were obtained. They are also given in table 1.The measured values coincide well with the values found in literature. The differences in refractive indices are smaller than 12%, while differences of the absorptivities at zero degree incidence angle are smaller than 4 % (cf. Qin et al., 2012, Querry, 1985).

Table 1. Exemplary measurements of absorptivities and refractive indices for polished copper and steel

Material	Wavelength in nm	Absorptivity at 0° incidence angle	Real part of the refractive index	Imaginary part of the refractive index
Cu-ETP Pure Copper 99.9 %	532	40 ± 2 %	0.79 ± 0.02	2.16 ± 0.03
Steel St 1.4301 AISI/SAE grade 304	532	35 ± 2 %	1.96 ± 0.05	3.66 ± 0.05
Steel St 1.4301 AISI/SAE grade 304	1064	29 ± 2 %	2.93 ± 0.11	5.04 ± 0.09

2.3. Efficiency

2.3.1. Residual energy coefficient

The calorimetric methods allows to determine η_{res}. If this value is close to unity, the drilling process is not very efficient since most of the applied energy is remaining within the workpiece. Although it might be used for bond breaking, the material is not ejected out in an efficient way. If η_{res} is close to zero, most of the applied energy is leaving the material. In this case, the bond breaking is also followed by an efficient removal of the heated material.

2.3.2. Breakthrough times

The time to drill through material of defined thickness was measured by using two photo diodes (Thorlabs DET10A/M). One was aligned to point at the top surface of the metal sheet to be drilled, while the other was aligned to point at the bottom surface of the sample. When the drilling process starts, the upper photo diode yields a signal, while at the time of break through the bottom photo diode yields a signal. The time for drilling through a sample was given by the time difference of the two signals. The sample thickness itself was measured with a caliper.

3. Experimental results and discussion

In Fig. 2, the residual energy coefficient (top) and the number of pulses to drill through a steel plate (bottom) are given as a function of the achieved drilling depth. The breakthrough times were measured as described in the previous section. The experiments have been performed for different repetition rates at the constant pulse energy of 215 µJ. This results in a mean fluence (Gaussian beam profile) of 68 J/cm². The repetition rates were varied between 10 kHz and 300 kHz. All drilled holes showed circular entrance diameters with values of 80 ± 10 µm (cf. Fig. 3).

3.1. Residual energy coefficient

During laser percussion drilling, the hole depth increases when the fluence at the bottom of the hole exceeds the ablation threshold. It has been shown in 2014 by Bauer et al. that for the ablation process of steel the residual energy coefficient at fluences of up to 8 times the threshold lies between 34 and 38 %. If the local fluence is below the ablation threshold, 100 % of the absorbed energy remains within the material, i.e. $\eta_{res} = 1$. The typical percussion drilling geometry is of parabolic shape at the beginning of the drilling process and changes into conical shape for deep hole drilling (cf. Döring et al., 2010). The total area on the inner walls of conical geometries increases linearly with depth. Therefore, the available fluence on the inner walls of a drilling hole should decrease linearly with depth. In the tip of the hole, the fluence also decreases but can be much higher than the ablation threshold due to multiple reflections (cf. Qin et al., 2012). This means that during an ongoing drilling process η_{res} in the slightly rounded tip of the hole should stay in the range of 35 to 40 %, while on the walls η_{res}will be close to 1. The area within the hole impinged with fluences below the threshold will increase with hole depth. Hence, η_{res}also should increase with depth. This is actually the case for all repetition rates. For every drilling depth, η_{res} is higher for 300 kHz compared to all lower repetition rates. The curves of η_{res} for 30 kHz and 100 kHz lie in between those for 10 and 300 kHz.

3.2. Breakthrough times

The effects discussed above have a direct impact on the needed pulse number N_P to drill through a steel plate, which is given in Fig. 2 (bottom). N_P was determined by averaging over a minimum of 5 drilling processes, the estimated error of N_P is smaller than 8 % and is not plotted for the sake of clarity.

As can be seen in Fig. 2 (bottom), for thicknesses between 0.2 mm and 1 mm and a repetition rate of 300 kHz, N_P is smaller – up to a factor of 10 for 0.4 mm – compared to the other repetition rates. While for a repetition rate of 10 kHz $N_P$is smaller for 0.1 mm and 0.2 mm, for 0.4 mm to 1 mm thickness it is equal for 10 kHz, 30 kHz, and 100 kHz.

For the maximum thickness of 1.5 mm the drilling process with 100 kHz seems to be the most productive. On the other hand, using 10 kHz or 300 kHz leads to higher N_P. One should keep in mind that for 10 kHz a pulse number of one million pulses equals to a drilling time of 100 s, while for 300 kHz this is a very fast process which lasts only 3 s. For 100 kHz, the number of needed pulses is smaller (around 300 thousand pulses) and therefore also results in a drilling time of 3 s, while still resulting in a high quality of the entrance of the drilled hole. In comparison, this is the optimum working point for the examined parameters.

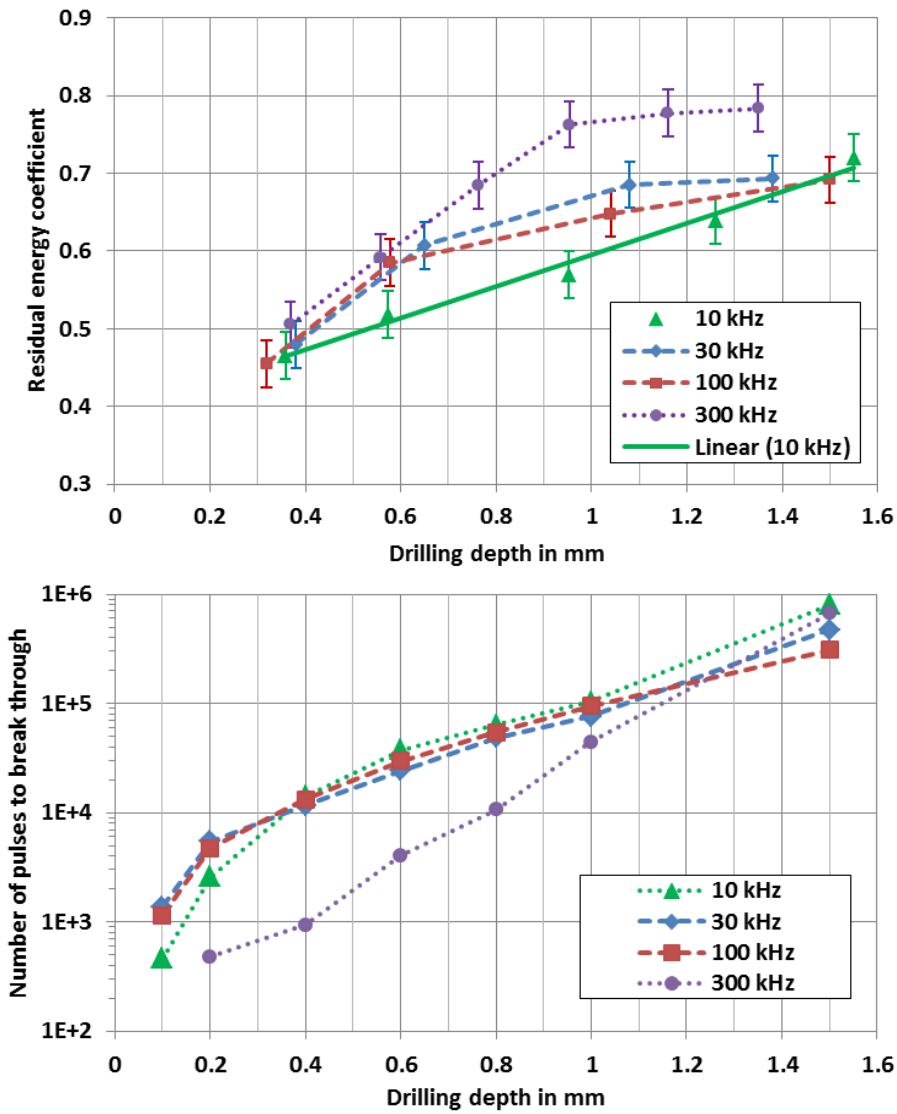

Fig. 2. Residual heat as a function of drilling depth (top) and number of pulses to break through as a function of the drilling depth in mm (bottom)

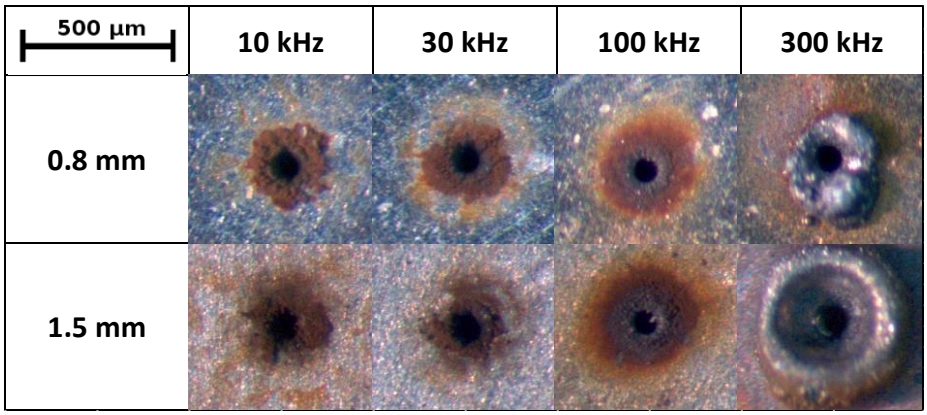

Fig. 3. Typical views of the entrance of the drilled holes for different thicknesses and repetition rates.

In conclusion, a drilling process completely free of pulse-to-pulse effects, which are mainly attributed to be heat accumulation effects, is not wanted in order to be able to keep the breakthrough times low. On the other hand, heat accumulation effects have to be suppressed as far as possible in order to keep the hole quality high.

4. Conclusions and outlook

In this paper we presented results from the determination of η_{res} and drilling-though times for laser percussion drilling. η_{res} lies between 40% and 70% for repetition rates of 10, 30 and 100 kHz, while it increases up to 80% for 300 kHz. For low repetition rates below about 10 kHz heat accumulation effects only play a minor role, for higher repetition rates of up to several 100 of kHz heat accumulation strongly affects the process. This can be also seen by investigating the breakthrough times for different thicknesses, which might serve as an indicator for the process efficiency. The number of pulses for drilling through steel plates can be decreased by slight heat accumulation effects in the case of 100 kHz, while for 300 kHz the strong heat accumulation leads to an increase of this characteristic time as well as low quality of the drilled hole.

Further research will concentrate on the investigation of the final hole geometry and the plasma expansion within the laser drilled holes.

References

Bauer, F., Michalowski, A., Kiedrowski, T., Nolte, S., 2015. Heat accumulation in ultra-short pulsed scanning laser ablation of metals. Opt. Express 23, 1035-1043

Bauer, F., Michalowski, A., Nolte, S., 2015. Residual Heat in Ultra-Short Pulsed Laser Ablation of Metals. Journal of Laser Micro/Nanoengineering Vol. 10, No. 3

Bulgakova, N.M. , Zhukov, V.P. , Vorobyev, A.Y. , Guo, C., 2008. Modeling of residual thermal effect in femtosecond laser ablation of metals: role of a gas environment. Appl. Phys. A 92: 883

Chichkov, B.N., Momma, C., Nolte, S., von Alvensleben, F., Tünnermann, A., 1996. Femtosecond, picosecond and nanosecond laser ablation of solids. Appl. Phys. A 63: 109.

Cheng, J., Liu, C.S., Shang, S., Liu, D., Perrie, W., Dearden, G., Watkins, K., 2013. A review of ultrafast laser materials micromachining, Optics & Laser Technology, Volume 46, pp. 88-102, ISSN 0030-3992

Döring, S., Richter, S., Nolte, S., Tünnermann, A., 2010. In situ imaging of hole shape evolution in ultrashort pulse laser drilling. Optics express 18.19 (2010): 20395-20400.

Hada, M.; Zhang, D.; Pichugin, K.; Hirscht, J.; Kochman, M. A.; Hayes, S. A.; Manz, S.; Gengler, R. Y. N.; Wann, D. A.; Seki, T.; Moriena, G.; Morrison, C. A.; Matsuo, J.; Sciaini, G.; Miller, R. J. D., 2014. Cold ablation driven by localized forces in alkali halides. Nature Communications 5, 3863

Loesel, F. H., Fischer, J. P., Götz, M.H. , Horvath, C., Juhasz, T., Noack, F., Suhm, N., Bille, J.F. 1998. Non-thermal ablation of neural tissue with femtosecond laser pulses. Applied Physics B: Lasers and Optics 66.1 (1998): 121-128.

Norm DIN EN ISO 11551:2004. Charakterisierung von Laserstrahlen und Laseroptiken.

Qin, Y, Michalowski, A. Weber, R., Yang, S., Graf, T., Ni, X., 2012. Comparison between ray-tracing and physical optics for the computation of light absorption in capillaries – the influence of diffraction and interference. Opt. Express 20, 26606-26617 (2012)

Querry, M. R., 1985. Optical constants, Contractor Report CRDC-CR-85034 (1985)

Vorobyev, A.Y., Guo, C., 2005. Direct observation of enhanced residual thermal energy coupling to solids in femtosecond laser ablation. Applied Physics Letters, 86,011916

Vorobyev, A.Y., Guo, C., 2005. Enhanced absorptance of gold following multipulse femtosecond laser ablation. Phys. Rev. B,72, 195422

Vorobyev, A., Kuzmichev, V., Kokody, N. P. Kohns, J. Dai, C. Guo., 2006. Residual thermal effects in Al following single ns- and fs-laser pulse ablation. Appl. Phys. A, 82: 357

Vorobyev, A.Y., Guo, C., 2006. Enhanced energy coupling in femtosecond laser-metal interactions at high intensities. Opt. Express 14, 13113-13119

Weber, R., Graf, T., Berger, P., Onuseit, V., Wiedenmann, M., Freitag, C., Feuer, A., 2014. Heat accumulation during pulsed laser materials processing. Opt. Express 22 (9), 11312–11324

Weber, R., Graf, T., Freitag, C., Feuer, A., Kononenko, T., Konov, V. I., 2017. Processing constraints resulting from heat accumulation during pulsed and repetitive laser materials processing. Optics Express 25.4 (2017): 3966-3979.

Yang, J., Zhao, Y., Zhang, N., Liang, Y., Wang, M., 2007. Ablation of metallic targets by high-intensity ultrashort laser pulses. Phys. Rev. B, 76, 16, 165430